AD-A114 246   UNITED TECHNOLOGIES RESEARCH CENTER EAST HARTFORD CT   F/G 20/5
               ELECTRON-BEAM SUSTAINED MERCURIC BROMIDE LASER STUDY.(U)
               APR 82   W L NIGHAN, R T BROWN   N00014-80-C-0247
UNCLASSIFIED   UTRC/R82-925096-1   NL

END
DATE
FILMED
6 -82
DTIC

R82-925096-1

Electron-Beam Sustained Mercuric Bromide Laser Study

Final Report
April 29, 1982

Prepared by
William L. Nighan and Robert T. Brown

United Technologies Research Center
East Hartford, Connecticut 06108

Accession For	
NTIS GRA&I	☒
DTIC TAB	☐
Unannounced	☐
Justification	
By	
Distribution/	
Availability Codes	
	Avail and/or
Dist	Special
A	

DTIC
COPY
INSPECTED
2

SECURITY CLASSIFICATION OF THIS PAGE *(When Data Entered)*

REPORT DOCUMENTATION PAGE		READ INSTRUCTIONS BEFORE COMPLETING FORM
1. REPORT NUMBER R82-925096-1	2. GOVT ACCESSION NO. AD-A11423H6	3. RECIPIENT'S CATALOG NUMBER
4. TITLE *(and Subtitle)* Electron-Beam Sustained Mercuric Bromide Laser Study		5. TYPE OF REPORT & PERIOD COVERED Final Report Mar. 1, 1980 – April 29, 1982
		6. PERFORMING ORG. REPORT NUMBER R82-925096-1
7. AUTHOR(s) William L. Nighan and Robert T. Brown		8. CONTRACT OR GRANT NUMBER(s) N00014-80-C-0247
9. PERFORMING ORGANIZATION NAME AND ADDRESS United Technologies Research Center Silver Lane East Hartford, CT 06108		10. PROGRAM ELEMENT. PROJECT. TASK AREA & WORK UNIT NUMBERS
11. CONTROLLING OFFICE NAME AND ADDRESS Office of Naval Research Physics Program Office 800 N. Quincy St., Arlington, VA 22217		12. REPORT DATE April 29, 1982
		13. NUMBER OF PAGES 47
14. MONITORING AGENCY NAME & ADDRESS(*if different from Controlling Office*)		15. SECURITY CLASS. *(of this report)* Unclassified
		15a. DECLASSIFICATION DOWNGRADING SCHEDULE

16. DISTRIBUTION STATEMENT *(of this Report)*

Approved for public release; distribution unlimited.
Reproduction in whole or in part is permitted for any purpose of the United
States Government.

17. DISTRIBUTION STATEMENT *(of the abstract entered in Block 20, If different from Report)*

18. SUPPLEMENTARY NOTES

This final report is based on a manuscript which has been submitted for
publication in the Journal of Applied Physics.

19. KEY WORDS *(Continue on reverse side if necessary and identify by block number)*

HgBr Laser, HgBr$_2$ Dissociation Laser, HgBr/HgBr$_2$ Laser Kinetics, E-Beam
Controlled HgBr Laser, Electron-HgBr$_2$ Collision Processes, HgBr$_2$ Electronic
Cross Sections

20. ABSTRACT *(Continue on reverse side if necessary and identify by block number)*
Results are reported of an investigation of fundamental kinetic processes
influencing discharge and laser properties typical of the 502 nm HgBr(B$\to$X)/
HgBr$_2$ dissociation laser. Specific attention is focused on conditions repre-
sentative of electron-beam controlled discharges. Experimental results and
corresponding analysis and interpretation are presented for several laser mix-
tures, focusing particularly on the factors affecting discharge characteristics
and HgBr(B) formation. A set of electron-HgBr$_2$ cross sections inferred on the

DD $_{1\ JAN\ 73}^{FORM}$ **1473** EDITION OF 1 NOV 65 IS OBSOLETE

S/N 0102-LF-014-6601

basis of analysis of experimental observations is presented, along with a discussion of the effect of electron-electron collisions on medium properties at the level of fractional ionization typical of the HgBr(B)/HgBr$_2$ laser.

PREFACE

Under the present contract United Technologies Research Center has carried out an experimental and theoretical investigation of the fundamental kinetic processes in an electron-beam-controlled, discharge-excited $HgBr(B \to X)/HgBr_2$ dissociation laser operating at 502 nm. This final report presents experimental results and corresponding analysis and interpretation for several laser mixtures, focusing particularly on the factors affecting discharge characteristics and $HgBr(B)$ formation. A set of electron-$HgBr_2$ cross sections inferred on the basis of analysis of experimental observations is presented, along with a discussion of the effect of electron-electron collisions on medium properties at the level of fractional ionization typical of the $HgBr(B)/HgBr_2$ laser.

During the time period of this contract, a significant evolution of the kinetic understanding of the $HgBr(B \to X)$ laser has taken place, based on work at UTRC and at other laboratories. Early in the present study, work at UTRC emphasized demonstration of the $HgBr(B \to X)$ laser in an e-beam sustained mode and resulted in the first published results demonstrating efficient laser operation using $Xe/HgBr_2$ mixtures (Appendix I). Under the second phase of this contract, emphasis has been placed on improving understanding of the $HgBr(B \to X)$ system and on seeking ways to enhance the laser efficiency and discharge stability beyond the levels demonstrated in earlier work. As the kinetic understanding has improved, it has become clear that direct electron excitation of $HgBr_2$ (a process previously thought to be insignificant) dominates $HgBr(B)$ formation for many conditions of interest. Because this formation process tends to be strongly dependent on discharge voltage, and is intimately coupled to the ionization kinetics, attempts to enhance $HgBr(B \to X)$ laser performance via temporal tailoring of experimental parameters (e.g., E/n tailoring) were not successful. Nonetheless, this work has helped to clarify understanding of kinetic processes in the $HgBr(B \to X)$ laser and should be of considerable value in carrying out device optimization and design studies within the constraints imposed by the various kinetic processes.

The present investigation was closely coordinated with other complementary Corporate and Navy supported experimental and theoretical programs, particularly Contracts N00014-80-C-0253 and N00014-76-C-0847. This report is based on a manuscript which has been submitted for publication to the Journal of Applied Physics.

R82-925096-1

Electron-Beam Sustained Mercuric Bromide Laser Study

TABLE OF CONTENTS

I. INTRODUCTION

The blue/green 502 nm HgBr(B→X) laser is a leading candidate for applications requiring an efficient (>1%) visible laser capable of generating relatively high average power (>100W)[1]. Efficient HgBr(B→X) oscillation has been demonstrated recently[2,3] using a variety of discharge excited mixtures containing 0.2–1.0% mercuric bromide, $HgBr_2$. Under such conditions the excited mercurous bromide molecule, HgBr(B), is produced as the result of dissociative excitation of $HgBr_2$ by either electron impact or reactive quenching of certain excited atoms or molecules[4].

In this paper we report the results of an investigation of fundamental kinetic processes influencing both discharge and laser properties typical of the HgBr(B)/$HgBr_2$ system. Specific attention is focused on conditions representative of electron-beam controlled discharges, an excitation method capable of generating high pressure, volume dominated glow discharges that are quasi-steady. Because of these characteristics, such discharges can provide a rich source of fundamental information difficult to obtain by other means[4]. Section II presents a description of the electron-beam controlled discharge experiment and related diagnostic apparatus, along with examples of representative current, voltage and fluorescence characteristics. A detailed discussion of our analysis of these characteristics is presented in Section III. Therein attention is focused on charged particle production and loss processes and their influence on the dependence of discharge current density on variations in applied electric field. The factors affecting HgBr(B) formation are treated in Sec. IV, wherein the effects of gas mixture variation are analyzed and a comparison of measured and computed

1

values of 502 nm gain discussed. This investigation and a related study[5] have shown that virtually all aspects of electron-$HgBr_2$ collision phenomena affect laser/discharge performance. The discussion of Section V deals with this aspect of the subject, focusing particularly on electron-$HgBr_2$ collision processes such as vibrational and electronic excitation. Therein a set of electron-$HgBr_2$ cross sections inferred on the basis of analysis of experimental observations is presented, along with a discussion of the role of electron-electron collisions for conditions typical of $HgBr(B)/HgBr_2$ laser discharges.

II. ELECTRON BEAM CONTROLLED DISCHARGE EXPERIMENTS

A. Discharge Cell

The present experiments were carried out using an e-beam controlled discharge having a 1.5 cm x 1.7 cm x 50 cm active volume, enclosed within a heated chamber as shown in Fig. 1. Because of the reactive nature of $HgBr_2$, proper cell design was critical in order to maintain purity of the gas mixtures and to minimize surface reactions. In the cell used in this investigation, the only materials in contact with the $HgBr_2$-containing gas mixture were type 316 stainless-steel, Pyrex, Viton, and dielectric coated mirrors. $HgBr_2$ crystals were contained in a Pyrex reservoir positioned in a side-arm as shown in the figure. The main cell structure was maintained at a temperature of 195°C; and variation of the reservoir temperature in the 150-190°C range provided a corresponding variation in $HgBr_2$ partial pressure from approximately 1 to 12 Torr[6]. The electron beam system and discharge driver are described elsewhere[2].
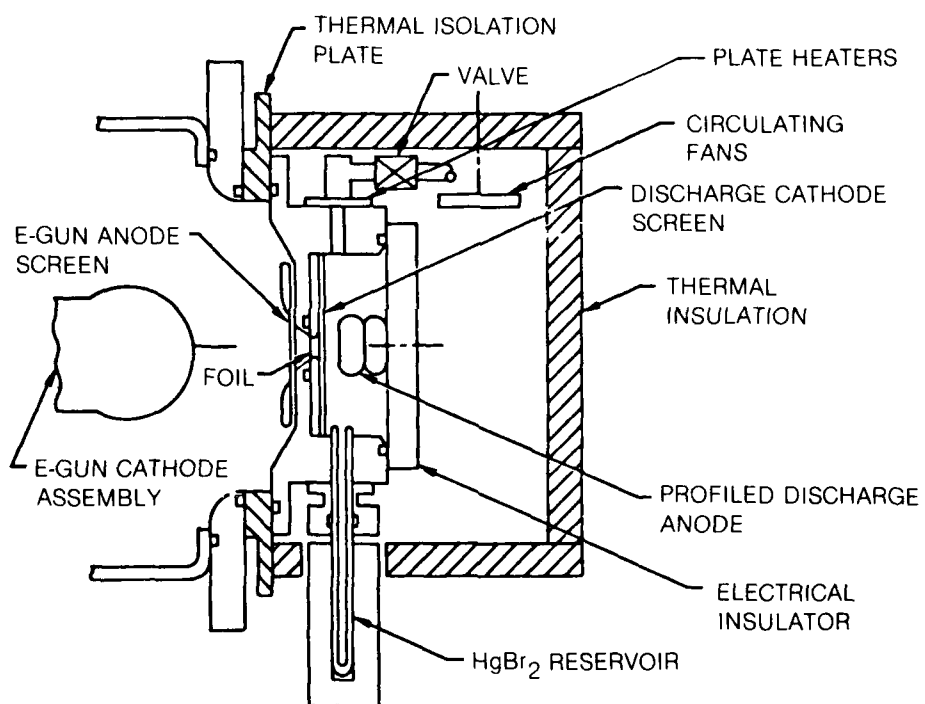
2

THERMAL ISOLATION PLATE

VALVE

PLATE HEATERS

CIRCULATING FANS

DISCHARGE CATHODE SCREEN

E-GUN ANODE SCREEN

THERMAL INSULATION

FOIL

E-GUN CATHODE ASSEMBLY

PROFILED DISCHARGE ANODE

ELECTRICAL INSULATOR

$HgBr_2$ RESERVOIR

Fig. 1   Schematic illustration of the heated $HgBr(B)/HgBr_2$ e-beam controlled laser discharge cell.

82-4-44-1

3

The discharge voltage was provided by a low inductance capacitor of a size so as to produce only a very slight decrease in voltage (i.e., E/n) during the pulse. Additionally, the electron-beam was initiated 200 nsec prior to the onset of the discharge voltage, and provided a constant e-beam current density of 0.5 Acm^{-2} for 1.2 μs. With this arrangement it was possible to produce a highly uniform plasma medium that was essentially quasi-steady, a circumstance greatly facilitating detailed comparison of experimental observations with the predictions of our discharge/laser kinetics model.

1. V-I Characteristics

In the work reported here, all measurements were carried out with a reservoir temperature of 170°C at a total cell pressure of 2.0 atm. Both neon and argon were used as buffers, with and without the addition of 5-10 % of an excitation transfer species such as N_2 and/or Xe. In order to ensure true quilibrium between the $HgBr_2$ density and the reservior temperature, the desired $HgBr_2$ density was established in the pre-evacuated cell prior to the admission of the buffer gas mixture. For each gas mixture, shots were made over a range of applied voltages, starting at a level below that for which any significant HgBr(B→X) fluorescence was observed and proceeding to the point at which nearly instantaneous discharge instability occurred.

Presented in Fig. 2 are representative voltage, current and fluorescence data for Ne containing 0.35% $HgBr_2$, corresponding to E/n values for which the fluorescence was relatively intense. For the lower E/n value a stable, uniform
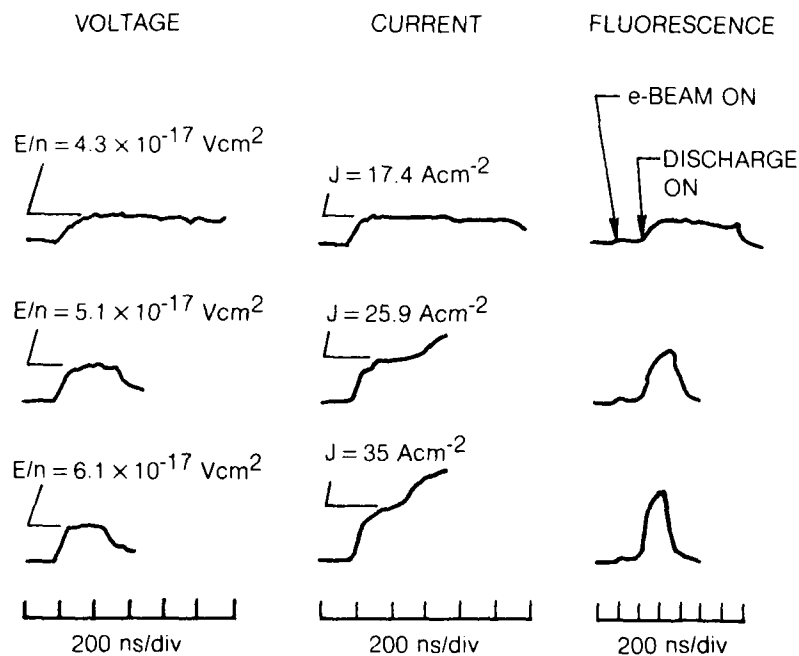
4

VOLTAGE   CURRENT   FLUORESCENCE

e-BEAM ON

$E/n = 4.3 \times 10^{-17}$ Vcm^2

$J = 17.4$ Acm^{-2}

DISCHARGE ON

$E/n = 5.1 \times 10^{-17}$ Vcm^2

$J = 25.9$ Acm^{-2}

$E/n = 6.1 \times 10^{-17}$ Vcm^2

$J = 35$ Acm^{-2}

200 ns/div   200 ns/div   200 ns/div

Fig. 2   Representative voltage, current and HgBr (B→X)
fluorescence characteristics for an e-beam controlled dis-
charge excited Ne − 0.35% HgBr$_2$ mixture at a pressure of
2 atm and a cell temperature of 190°C.   The e-beam current
density, at 0.5 Acm^{-2}, was constant for 1.2 μs, and was
initiated 200 ns prior to application of the discharge
voltage.

5

discharge could be maintained for 1 μs until the e-beam was terminated. However, as E/n was increased the discharge and fluorescence terminated prematurely due to the occurrence of ionization instability[2,7]. This general behavior was four' to be typical of all mixtures and conditions examined.

B. Gain Measurement

In order to obtain a quantitative relationship between the relative fluorescence and the HgBr(B) density, and to relate discharge current, voltage, and fluorescence to measured laser performance, the arrangement shown in Fig. 3 was used to make small-signal gain measurements. A nitrogen-pumped dye laser (Molectron model DL-14) was used in a standard two-beam configuration with the probe and reference pulse energies detected using pyroelectric joulemeters (Molectron model J3). A photodetector was used to monitor the superimposed fluorescence and probe laser signals, and to verify the temporal location of the probe pulse. Since the probe pulse was short (∿5 nsec) compared to the discharge duration, shot-to-shot measurements were used to determine the temporal variation of the gain during the discharge pulse. In the present study all small-signal gain data were obtained at 502.2 nm (i.e., at the wavelength exhibiting strongest lasing when the discharge was operated with an optical cavity).

Detailed gain measurements were carried out for selected gas mixtures and discharge voltages. Qualitatively, the present studies yielded results in good agreement with those reported by other investigators[3], and showed that relative changes in measured small signal gain correlated very closely with variations in
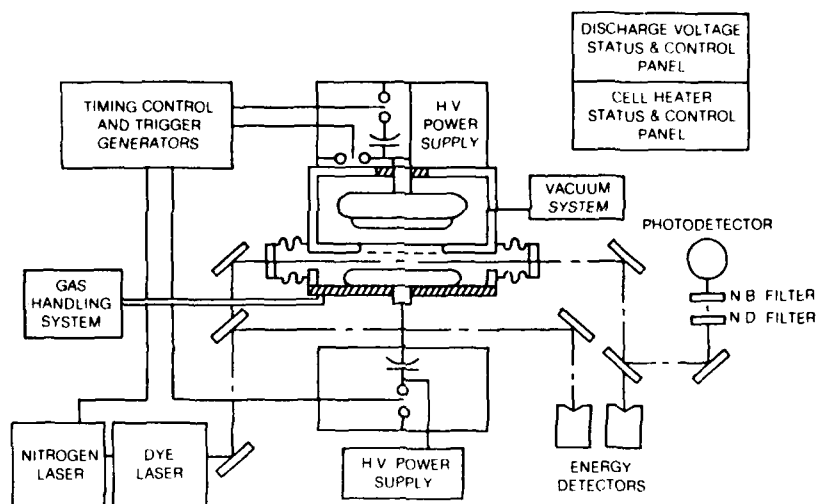
DISCHARGE VOLTAGE
STATUS & CONTROL
PANEL

CELL HEATER
STATUS & CONTROL
PANEL

TIMING CONTROL
AND TRIGGER
GENERATORS

H V
POWER
SUPPLY

VACUUM
SYSTEM

PHOTODETECTOR

GAS
HANDLING
SYSTEM

N B FILTER
N D FILTER

NITROGEN
LASER

DYE
LASER

H V POWER
SUPPLY

ENERGY
DETECTORS

Fig. 3   Diagram of small-single gain experiment   and
related apparatus.

82—4—44—2

relative fluorescence. On the basis of these findings, the fluorescence data

were interpreted as relative small signal gain, even for gas mixtures and

voltage ranges for which gain measurements were not actually carried out.

III. DISCHARGE KINETICS

A. Analysis of V-I Variations

Although accurate measurement of discharge voltage and current is relatively

straightforward for conditions typical of those presented in Fig. 2, quantitative

computation of these properties is quite difficult, even though the e-beam con-

trolled discharge medium closely approximates a quasi-steady, spatially uniform

medium. Accurate prediction of the variation of discharge current density, J,

with E/n requires knowledge of the electron drift velocity and all important

charged particle production and loss processes. Depending on mixture conditions,

the drift velocity is very sensitive to low energy electron-$HgBr_2$ collision

processes such as vibrational and electronic excitation,[5] and to the effect of

electron-electron collisions on the electron energy distribution function,[7] a

topic to be discussed in Sec. V. Although charged particle production is dominated

by the e-beam source for low E/n values, direct and multistep ionization by low

energy discharge electrons invariably become important as E/n is increased,

ultimately resulting in discharge instability. Both $HgBr_2$ dissociative attachment

and electron-ion recombination are found to contribute to the loss of electrons

for the conditions of interest.

1. Computed Drift Velocity and Attachment Coefficient

Presented in Figs. 4 and 5 are electron drift velocities and attachment coefficients for the mixtures examined in this investigation, computed[8] using reported cross sections for Ne,[9] Xe,[10] N_2[11] and for $HgBr_2$[5]. Clearly there are substantial mixture-to-mixture variations in the drift velocity over the 1-10 Td E/n range. Figure 5 indicates that the attachment coefficient is less sensitive to mixture variation, with the exception of mixtures containing N_2. In the latter case the resonance in the e-N_2 vibrational cross sections near 2.0 eV truncates the electron energy distribution,[11] so that there are very few electrons with energy above the 3.1 eV threshold for dissociative attachment[5]. Thus, for low E/n values the $HgBr_2$ attachment coefficient is unusually low with N_2 in the mixture.

2. J vs E/n Variation

Measured and computed variations of discharge current density with E/n are presented in Figs. 6 and 7 for Ne and Ar containing 0.35% $HgBr_2$, and for Ne-0.35% $HgBr_2$ mixtures containing either 5% N_2 or 10% Xe. Both measured and computed values refer to a time 200 ns after application of the discharge voltage pulse. For these conditions the ratio of discharge power input to that of the e-beam ranges from about two to twenty for the Ne, Ar, and Ne + Xe-$HgBr_2$ mixtures; and from twenty to sixty for the Ne - N_2 - $HgBr_2$ mixture, reflecting the high current density and E/n values typical of the latter. Calculations show that for the lowest E/n values in all four mixtures the only ionization is provided by the electron-beam, either directly or by way of Penning ionization reactions. In mixtures not containing N_2 the principle electron loss process is dissociative
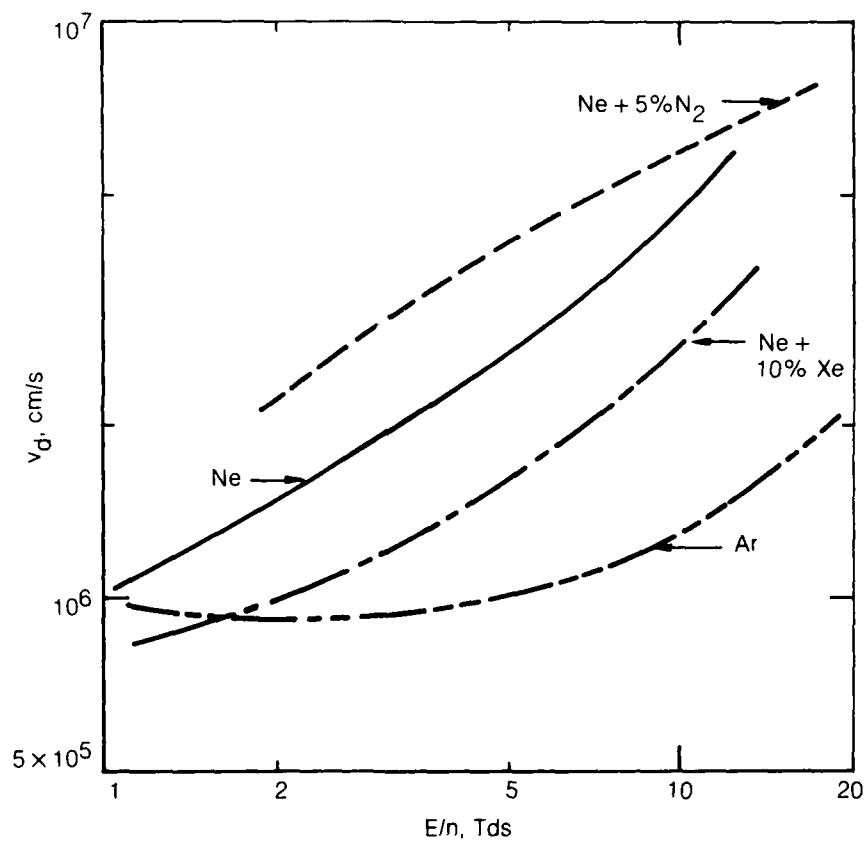
9

Fig. 4   Computed electron drift velocity for the indicated
mixtures containing 0.35% HgBr$_2$. The drift velocity (and
the electron energy distribution function) was computed for
a fractional ionization level of 2 x 10^{-6} using the cross
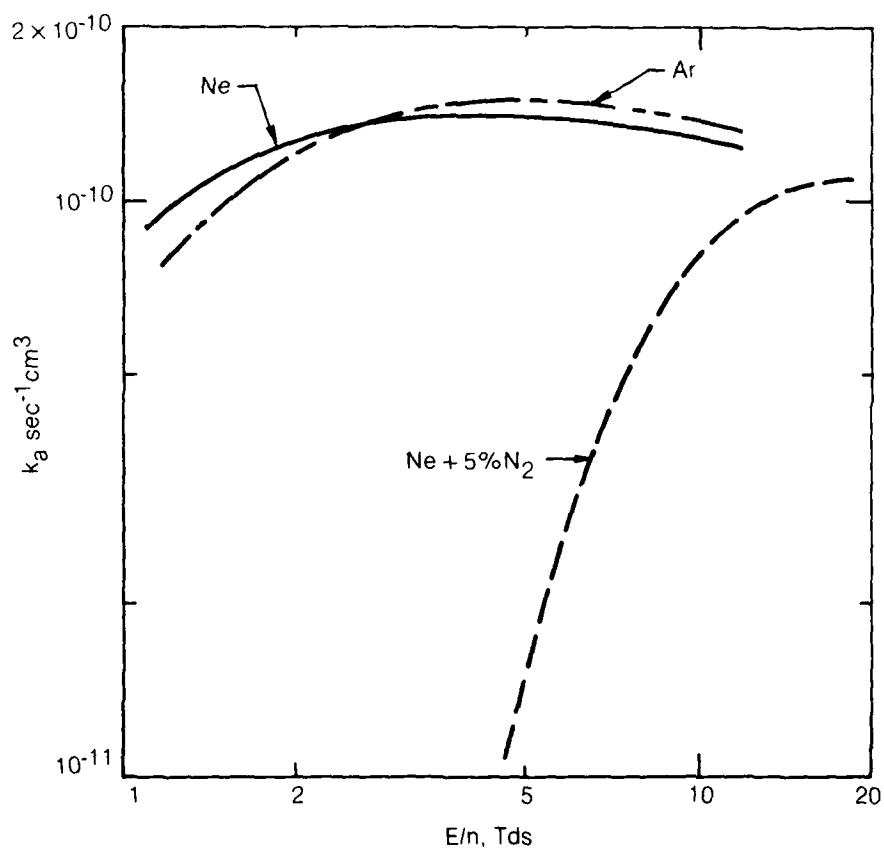sections shown in Fig. 12 as discussed in Sec. V.

Fig. 5 Computed electron – HgBr$_2$ dissociative attachment
coefficients for the conditions of Fig. 4. The attachment
coefficient for the Ne-Xe-HgBr$_2$ mixture falls between the
curves for the Ne and Ar mixtures, and has been omitted
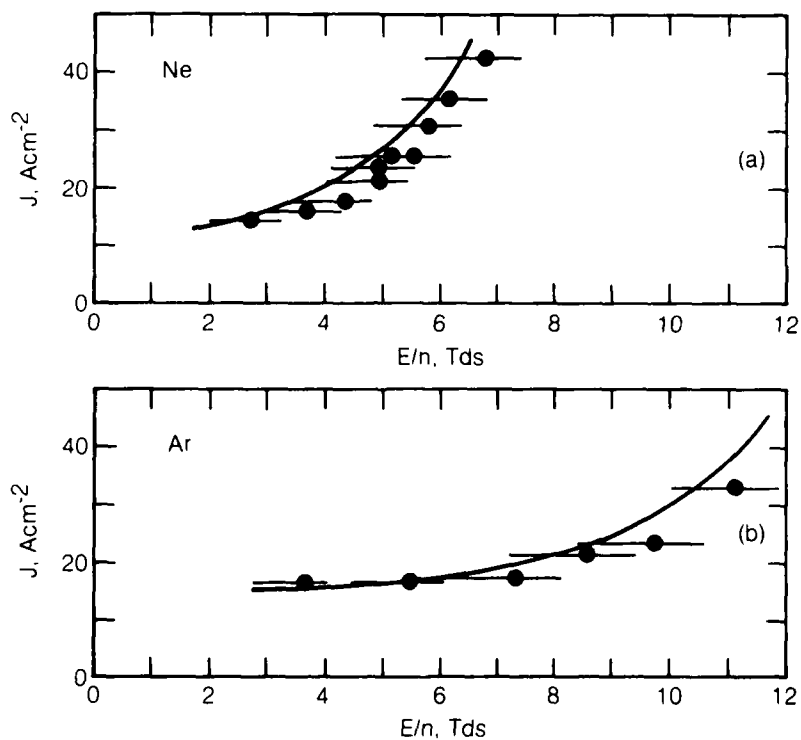for the sake of clarity.

82—4—44—5

11

Fig. 6 Measured and computed discharge current density
for Ne (a) and Ar (b) containing 0.35% HgBr$_2$ at the cell
conditions of Fig. 2. Because medium properties are par-
ticularly sensitive to variations in E/n the uncertainty
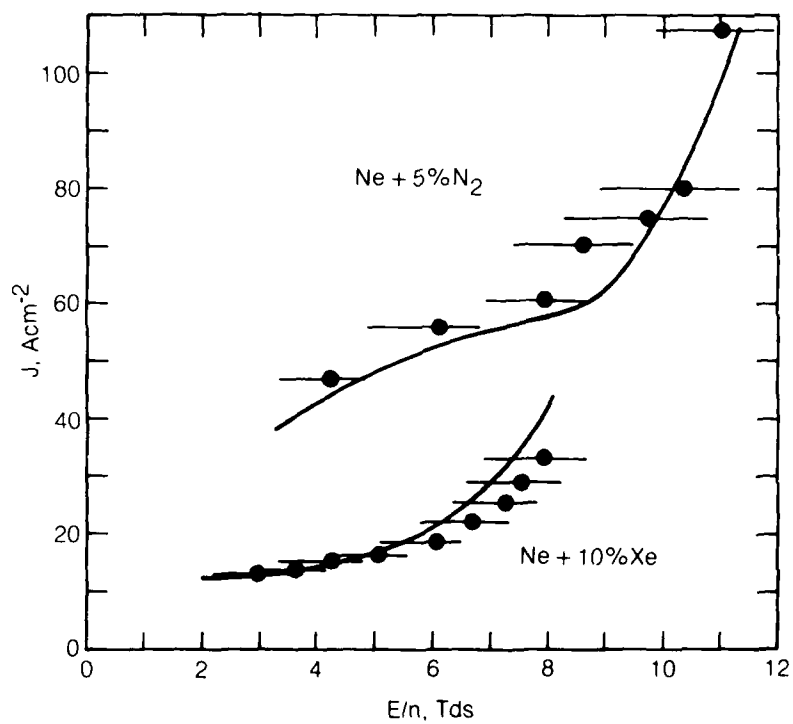in the measured values of this parameter is indicated.

12

Fig. 7   Measured and computed discharge current density for
a Ne - 5% N_2 mixture and a Ne - 10% Xe mixture, both con-
taining 0.35% $HgBr_2$, and cell conditions otherwise similar
to those of Figs. 2 and 6.

13

attachment, with electron-ion recombination representing between 25 and 50% of the total loss depending on specific conditions. Thus, for low E/n values the agreement between the measured and computed current density, along with mixture-to-mixture consistency, is indicative of the accuracy with which the electron drift velocity and attachment coefficients can be computed (Figs. 4 and 5).

Examination of Figs. 6 and 7 shows that the current density increases as E/n is increased for all mixtures, as expected. However, the data exhibit substantially different variations, primarily indicative of the dependence of the drift velocity on E/n (Fig. 4), and on the increasing importance of direct and multistep ionization at higher E/n values. For the Ar-HgBr$_2$ mixture and the Ne-HgBr$_2$ mixture containing Xe, the present calculations show that the sharp rise in the current density, ultimately resulting in discharge instability, is a consequence of multistep ionization of the metastable and higher excited states[7] of Ar and Xe, respectively. In contrast to this situation, direct electron impact ionization of HgBr$_2$ dominates in the Ne-HgBr$_2$ mixture with or without N$_2$ present. Whether dominated by multistep or direct ionization, the calculated E/n for instability onset was found to be in good agreement with experimental observations for all mixtures examined.

3. Electron-Ion Recombination

Because attachment is not significant for low E/n values in the mixture containing N$_2$, the measured current density in this case provides a means for determining an effective electron recombination coefficient for HgBr$_2$ related ions. The present modeling of ion species concentrations included the ions

Ne^+, Ne_2^+, Ar^+, Ar_2^+, N_2^+, N_4^+, Xe^+, Xe_2^+, $HgBr_2^+$ and the product ions $HgBr^+$, Hg^+ and Br^+. For the conditions of Figs. 6 and 7 calculations indicate that $HgBr_2^+$ is usually dominant, followed by the sum of the indicated product ions. Satisfactory agreement between theory and experiment is obtained using a value of $2 \pm 1 \times 10^{-7} s^{-1} cm^3$ for the electron-ion recombination coefficient for all $HgBr_2$ related ions. This value is probably representative of $HgBr_2^+$, $HgBr^+$, and/or these ions clustered to $HgBr_2$[12], for average electron energy values in the 2-4 eV range.

IV. HgBr(B) FORMATION

A large number of $HgBr_2^*$ states[4,13] can be produced either by direct electron impact or by $HgBr_2$ reactive quenching of excited states of species such as Ne, Ar, N_2 and Xe. However, only the $^{3,1}\Sigma_u^+$ state of $HgBr_2$ predissociates to from $HgBr(B)$[13]. Further, available evidence indicates that this state can be produced in substantial quantity only by electrons and/or by the excited states of N_2[14,15] or Xe[14,16].

Figure 8 illustrates the general sequence of events resulting in HgBr(B) formation in discharge excited lasers. The large Franck-Condon shift between the B and X states of HgBr is such that the laser transitions terminate on high vibrational levels of the X state. These levels are rapidly deactivated by collisions with the background gas,[17] thereby permitting efficient optical extraction. Following laser oscillation the HgBr(X) state recombines with Br atoms to reform $HgBr_2$, the final step in a reaction sequence that appears to be nearly completely cyclic under carefully controlled conditions.
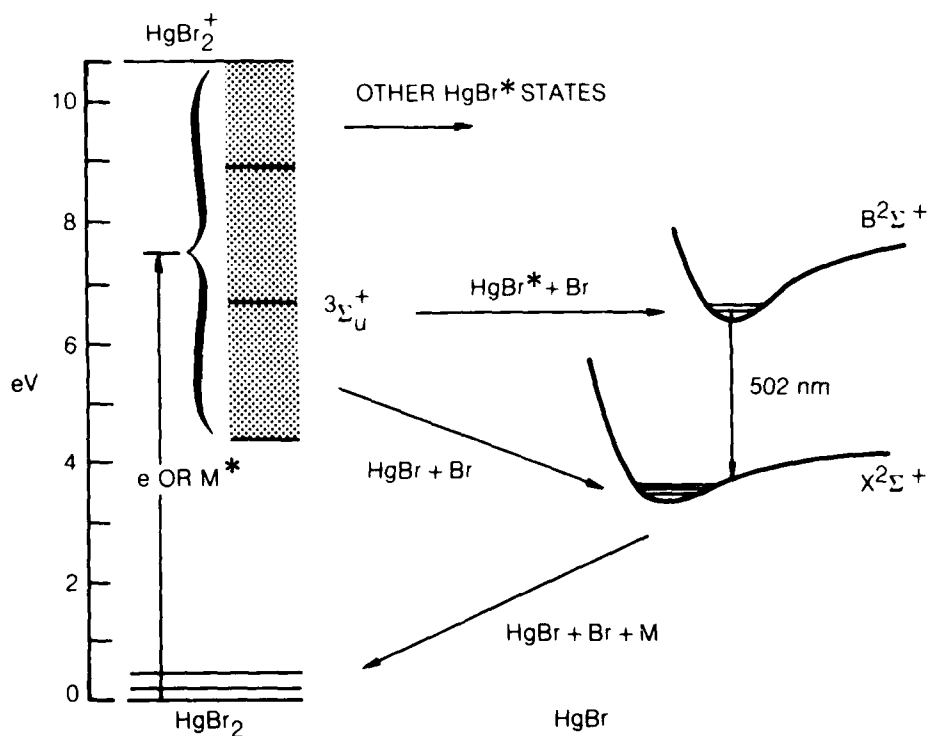
Fig. 8   Sequence diagram illustrating the dominant steps
in HgBr(B) formation in the $HgBr_2$ dissociation laser. Both
electrons (e) and certain excited species (M*) can excite
the $^{3,1}\Sigma_u^+$ states of $HgBr_2$ that predissociate to form HgBr(B).
In addition, many $HgBr_2$ states are excited which do not
yield HgBr(B) upon predissociation. The energy thresholds
at 5.0, 6.4 and 7.9 eV of the three effective $HgBr_2$ elec-
tronic cross sections (as discussed in Sec. V) are indi-
cat'd.

The laser/discharge medium produced using the e-beam controlled discharge excitation technique is especially well suited for evaluation of the HgBr(B) production reactions illustrated in Fig. 8. In order to study both electron impact excitation and excitation transfer reactions, HgBr(B) fluorescence and gain were examined for several mixtures over a range of discharge conditions.

A. Ne and Ar-HgBr$_2$ Mixtures

Neon and Ar both have been used as the background gas in the present study and by other investigators as well[3]. Although rare gas metastable atoms and higher excited states are produced both by the electron beam and by low energy electron collisions in such mixtures, reactive quenching of these species by HgBr$_2$ results in little or no HgBr(B) formation[14,16]. In the present analysis HgBr$_2$ quenching rate coefficients for the excited states of Ne and Ar have been taken to be 2×10^{-10} and 3×10^{-10} sec^{-1}cm^3, respectively. For Ne* quenching all the reaction products have been assumed to be ions, i.e., the products of Penning reactions, while for Ar* two thirds of the reaction species have been assumed to be ions and one third neutral fragments. Use of these values has been found to be consistent with the observed current-voltage characteristics (Fig. 6), contributing to the agreement between computed and measured values of current density, particularly at low E/n values.

Figure 9 shows the measured and computed values of small signal gain in Ne and Ar containing 0.35% HgBr$_2$. Under these conditions, analysis shows that HgBr(B) is produced as the result of direct electron impact dissociative excitation of HgBr$_2$. Clearly, the agreement between the computed and measured values of gain
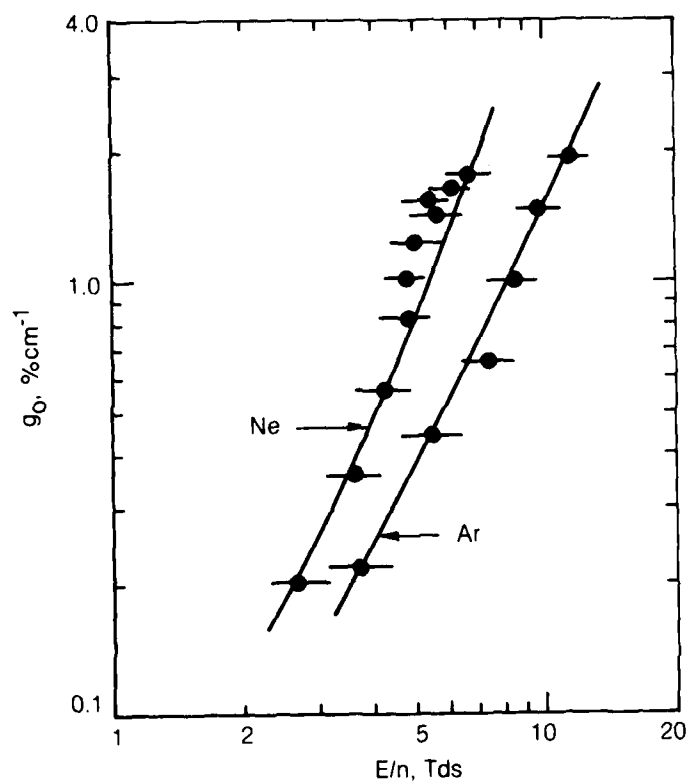
17

Fig. 9   Measured and computed small signal gain for Ne and
Ar containing 0.35% $HgBr_2$ excited under the e-beam controlled
discharge conditions of Figs. 2 and 6.

is good, lending support to the electron-$HgBr_2$ cross sections used in the calculation, a topic to be discussed in Sec. V. For the higher E/n values calculations show that the HgBr(B) formation efficiency for the Ne and Ar-$HgBr_2$ mixture conditions of Fig. 9 is in the 2.5-3.0% range.

In addition to direct electron excitation of $HgBr_2$, approximately a 5% contribution to the computed gain is the result of the recombination of $HgBr_2^+$ with electrons and Br^-, based on the assumption that the HgBr(B) branching fraction for such recombination reactions is 10%. This branching fraction is found to be sufficient to account for the barely observable fluorescence with e-beam excitation alone (Fig. 2). Under this circumstance recombination is likely to be the only significant process resulting in HgBr(B) production.

B. Ne-N_2-$HgBr_2$ Mixtures

With N_2 added to the Ne-$HgBr_2$ mixtures discharge and laser properties are changed dramatically, primarily as a consequence of N_2 vibrational and electronic excitation[11]. Of course direct electron excitation of $HgBr_2$ resulting in HgBr(B) still occurs, but calculations show that the magnitude of the rate coefficient for this reaction is reduced substantially from its value in a Ne-$HgBr_2$ mixture. Offsetting this decrease are excitation transfer reactions involving $N_2(A^3\Sigma_u^+)$ and higher N_2 excited states[15]. Unfortunately, the branching to HgBr(B) upon reactive quenching of $N_2(A)$ by $HgBr_2$ is only 15%. This reaction combined with direct electron dissociative excitation of $HgBr_2$ is insufficient to account for the gain observed in the N_2 mixture. However, electron excitation of $N_2(A)$ represents only
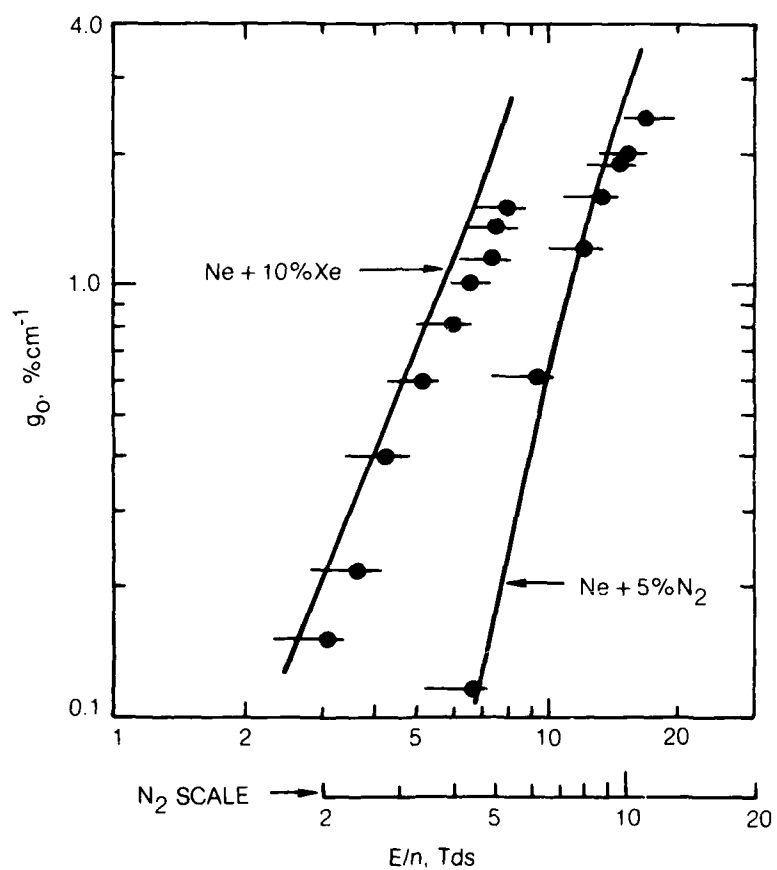
Fig. 10   Measured and computed small signal gain for a Ne –
10% Xe mixture and a Ne – 5% – N_2 mixture, both containing
0.35% $HgBr_2$, excited under the e-beam controlled discharge
conditions of Figs. 2 and 6.   Note that the E/n scale for
the N_2 mixture has been shifted for the sake of clarity.

82-4-44-10

20

20-40% of the total N_2 electronic excitation,[18] and there is evidence that a higher N_2 excited state(s) also contributes to HgBr(B) formation[15]. Thus, in the present analysis another N_2 excited state was considered in addition to $N_2(A)$.

1. N_2^*-HgBr$_2$ Branching to HgBr(B)

The rate coefficient for electron impact excitation of the higher energy N_2 electronic state was taken as the sum of those of nine other N_2 states for which cross sections have been reported[19]. Assuming that the total HgBr$_2$ quenching coefficient for this single _effective_ state is $2 \times 10^{-10} s^{-1} cm^3$, a value typical of $N_2(A)$, an HgBr(B) branching fraction of $25 \pm 5\%$ is found to result in satisfactory agreement between measured and computed gain as shown in Fig. 10. Most probably HgBr(B) is produced primarily as a consequence of an HgBr$_2$ reaction with $N_2(B^3\Pi_g)$;[18], the highly populated and closely coupled $B^3\Pi_g$ and $W^3\Delta_u$ states of N_2 being produced both by electron impact on ground state N_2 and by cascade from higher lying levels. For the conditions of the N_2 mixture of Fig. 10 approximately 80% of the HgBr(B) production results from N_2 excitation transfer (one third of that from $N_2(A)$), and 20% from direct electron impact excitation of HgBr$_2$. The computed HgBr(B) formation efficiency for the higher E/n values of Fig. 10 is in the 1.0-1.5% range.

C. Ne-Xe-HgBr$_2$ Mixtures

As is typical of the rare gases, the two lowest Xe(6s) states, $^3P_2$ and $^3P_1$, can be produced very efficiently in an e-beam controlled electric discharge. Additionally, these Xe states are strongly quenched by HgBr$_2$ resulting in HgBr(B) formation with an efficiency of about 80%[14,16]. For these reasons Xe would seem to be the ideal excitation transfer species for the HgBr(B)/HgBr$_2$ laser, and

initial calculations[2] indicated that the HgBr(B) formation efficiency in mixtures

containing Xe could be on the order of 10%. Unfortunately, such has not been

found to be the case. Indeed, the Xe–HgBr$_2$ laser mixtures examined to date

are not as efficient as others under e-beam controlled discharge excitation,

although their performance is comparable. Absorption in the blue/green region,

probably due to Xe$_2^*$, may contribute to a lower optical extraction efficiency; but

the explanation must lie elsewhere since the observed HgBr(B→X) fluorescence

is much less than predicted for Xe–HgBr$_2$ mixtures.

1. Xe* Kinetics

Figure 11 shows the Xe electronic levels of significance in the present

context. The two 6s states at about 8.3 and 8.5 eV are efficiently excited by

electron impact on ground state Xe, as are many higher lying Xe states. In the

present analysis it is assumed that the closely spaced $^3P_2$ and $^3P_1$ levels are

completely mixed by electron and neutral collisions and constitute a single

level. The 6s', 6p and all higher lying states are also closely coupled

together[20], and are assumed to be coupled to the lower energy 6s levels only by

electron collisions as indicated in the figure. In addition, the single, effec-

tive upper state (6s', 6p,...) so comprised is assumed to be strongly quenched by

HgBr$_2$ with no branching to HgBr(B). Even on the basis of these rather conserva-

tive assumptions the computed HgBr(B) fluorescence and formation efficiency are

found to be higher than measured values. Consideration of the factors contributing

to this situation shows that the underlying reason is a computed Xe(6s) population
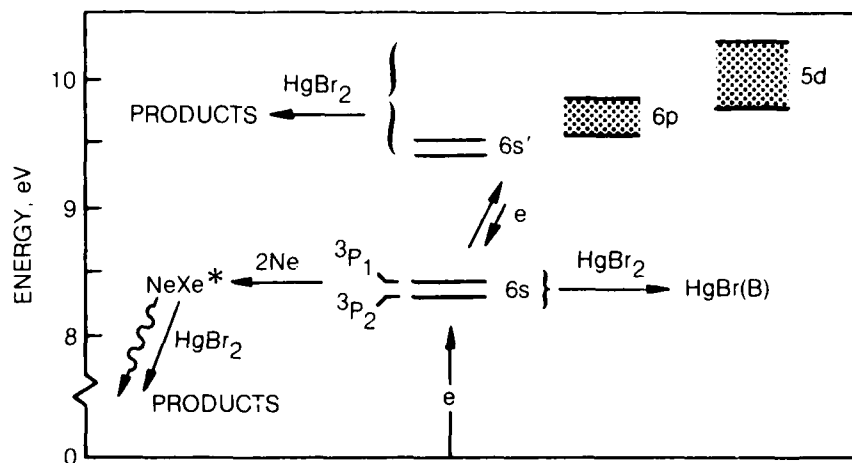
which is apparently too large.

Fig. 11 Simplified Xe energy level diagram showing the excited states of primary importance in the present context, and indicating the dominant production and loss processes for each group of states as discussed in the text.

23

2. Xe(6s) Three-body Quenching

Three-body quenching of Xe^* would, at first, seem to be insignificant for the conditions of this experiment given the relatively small ($\sim 10^{-32} s^{-1} cm^3$) rate coefficient for the reaction $Xe(^3P_2) + 2Xe \rightarrow Xe_2^* + Xe$, as measured by several investigators. Nevertheless, as an explanation of the observations discussed above, we propose a three-body quenching reaction acting selectively on the $Xe(^3P_1)$ state, thereby depleting the population of the coupled $^3P_1$ and $^3P_2$ levels. Measurements[21] indicate that the reaction $Xe(^3P_1) + Xe + Ar \rightarrow Xe_2(^1\Sigma_u^+)$ has a rate coefficient of $2 \times 10^{-31} s^{-1} cm^3$, a factor-of-ten times higher than the analogous $^3P_2$ reaction. Nevertheless, even with this value for the rate coefficient, merely substituting Ne as the third body has little effect on the computed Xe(6s) population for the present conditions because the Xe fractional concentration is only 10%. However, if it is assumed that two Ne atoms are involved, with the resultant $NeXe^*$ molecule decaying radiatively or being quenched by collisions with $HgBr_2$ on a time scale less than that typical of the reaction driving $NeXe^*$ back to $Xe(^3P_1)$, then reasonable agreement between computed and measured gain can be obtained. For example, the computed gain shown in Fig. 10 for the 10% Xe mixture was generated on this basis using a rate coefficient of $2 \times 10^{-31} sec^{-1} cm^6$ for the proposed three body $Xe(^3P_1) \rightarrow NeXe^*$ reaction. The hypothesis that three-body quenching of Xe^* in Ne proceeds at a rate much faster than suggested by the value of the rate coefficient measured for the $Xe(^3P_2)$ state alone is also consistent with recent observations[22] of increased $Xe(^3P_1)$ decay in Ne at lower pressures. Further, present understanding[16] of the reaction channel resulting in the formation of

HgBr(B) following quenching of $Xe(^3P_{2,1})$ by $HgBr_2$ suggests that the analogous reactions involving molecular species such as Xe_2^* and/or $NeXe^*$ are likely to have HgBr(B) branching fractions much less than unity.

Additional clarification of the factors controlling the $Xe(^3P_2)$ population in discharges of the type under consideration may provide the basis for devising means to take advantage of the highly efficient formation of HgBr(B) following reactive quenching of $Xe(^3P_2)$ by $HgBr_2$. Clearly, additional experimentation in this area would be most helpful.

V. ELECTRON COLLISION PROCESSES

A. Electron-HgBr$_2$ Electronic Cross Sections

Interpretation of the observed HgBr(B→X) fluorescence in e-beam controlled discharge excited mixtures with Ne or Ar as the buffer immediately leads to the conclusion that direct electron impact excitation of $HgBr_2$ is the dominant reaction leading to HgBr(B). Under these circumstances, the electron-ion recombination rate is insufficient to account for the observed blue/green fluorescence. Further, the dissociative attachment rate is also too low, and at low E/n values has a qualitative variation[5,23] inconsistent with that of the observed fluorescence. Thus, HgBr(B) is not the dominant neutral fragment of the e-HgBr$_2$ attachment reaction as once suggested[24]. On the other hand, a relatively modest rate coefficient (i.e., cross section) for dissociative excitation of $HgBr_2$, branching to H$_3$Br(B), easily accounts for the observed fluorescence. On this basis a cross section for HgBr(B) formation was inferred as part of the present investigation

and independently by McGeoch, Hsia and Klimek,[25] both by analyzing e-beam controlled laser discharge characteristics. The present cross section for HgBr(B) formatio·, $Q_x(B)$, as determined in this manner is shown in Fig. 12.

More difficult than determining the approximate magnitude and E/n variation of the e-HgBr$_2$ rate coefficient for HgBr(B) production, is generation of a self consistent set of companion cross sections representative of HgBr$_2$ vibrational[5] and electronic excitation, that are capable of predicting the mixture-to-mixture variation of discharge and laser properties in a satisfactory way. Cross sections for direct e-HgBr$_2$ vibrational excitation, Q_{VD}, with an energy loss of 0.035 eV, and for resonant vibrational excitation, Q_{VR}, with an effective energy loss of 0.25 eV, have been recently determined from an analysis of data obtained using an electron swarm experiment[5]. These cross sections are also shown in Fig. 12, along with those for HgBr$_2$ dissociative attachment and ionization[5,23]. In addition to $Q_x(B)$, two other e-HgBr$_2$ electronic cross sections have been used in this analysis, one having a threshold of 5.0 eV, $Q_x(5.0)$, the approximate threshold for HgBr$_2$ electronic excitation[13], and a higher energy cross section with a threshold of 7.9 eV, $Q_x(7.9)$. Of course there are many HgBr$_2$ electronic states[13] that can be excited by electrons, but for the present purposes use of three effective cross sections is sufficient to explain experimental observations of discharge/laser performance.

The magnitude of the electronic cross section, $Q_x(5.0)$, was adjusted so that, in combination with the resonant vibrational cross section, Q_{VR}, the low E/n behavior of HgBr(B) fluorescence computed using $Q_x(B)$ was in satisfactory agreement with experiment. As indicated in Fig. 8, the HgBr$_2$ 5.0 eV process results
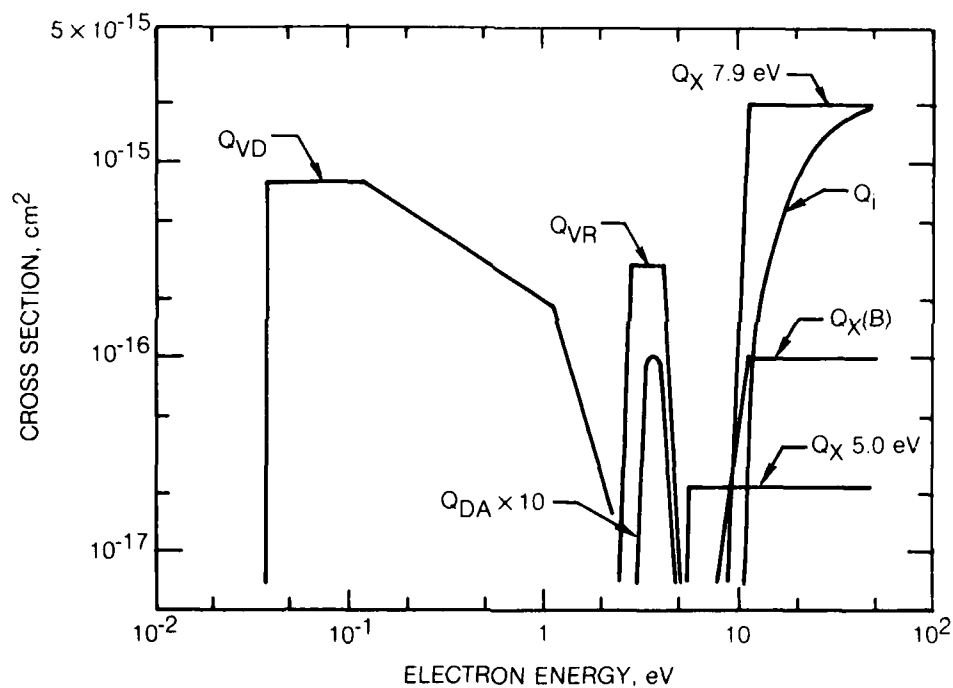
Fig. 12 Measured electron cross sections for HgBr$_2$ dissoc-
iative attachment, Q_{DA}, and ionization, Q_i, as reported in
Refs. 5 and 23, along with the cross sections for direct,
Q_{VD}, and resonant, Q_{VR}, vibrational excitation as inferred
from analysis of electron swarm experiments (Ref. 5). Also
shown are the electronic cross sections inferred as part of
the present investigation as discussed in Sec. V.

27

in HgBr(A,X) upon predissociation. However, a much larger cross section, $Q_x(7.9)$, most likely representative of a number of $HgBr_2^*$ states, is required to predict both discharge and fluorescence in agreement with experimental observation. This finding is in agreement with the observations of McGeoch, Hsia and Klimek,[25] and also with recently measured[26] electron energy loss spectra in $HgBr_2$, which indicate the existence of a large cross section with a corresponding energy loss of about 8.0 eV.

1. Attachment and Ionization in Ne-HgBr$_2$ Mixtures

Computed $HgBr_2$ attachment and ionization coefficients for the Ne-HgBr$_2$ mixture conditions discussed earlier are shown in Fig. 13, and serve to illustrate the importance of $Q_x(7.9)$. Since the threshold for electronic excitation of Ne is well above the 10.62 eV $HgBr_2$ ionization potential, in Ne-HgBr$_2$ mixtures the effect of electronic excitation of $HgBr_2$ alone determines the E/n value for which $HgBr_2$ ionization becomes important relative to attachment. Since the HgBr$_2$ cross sections for attachment and ionization are well known,[5,23] calculations show that the magnitude and energy variation of the cross section $Q_x(7.9)$ determines the E/n value for which the <u>net</u> attachment, $k_a - k_i$, begins to decrease rapidly leading to e-beam controlled discharge current runaway. In the present investigation, the magnitude and, more importantly, the slope of $Q_x(7.9)$ were adjusted until the E/n variation of discharge current density, including instability onset, could be predicted in Ne-HgBr$_2$ mixtures, along with the E/n variation of the gain based on $Q_x(B)$. The resulting $Q_x(7.9)$ so determined was also found to be consistent with observations in an electron swarm experiment[5] under conditions very different from those of the present e-beam controlled laser discharge.
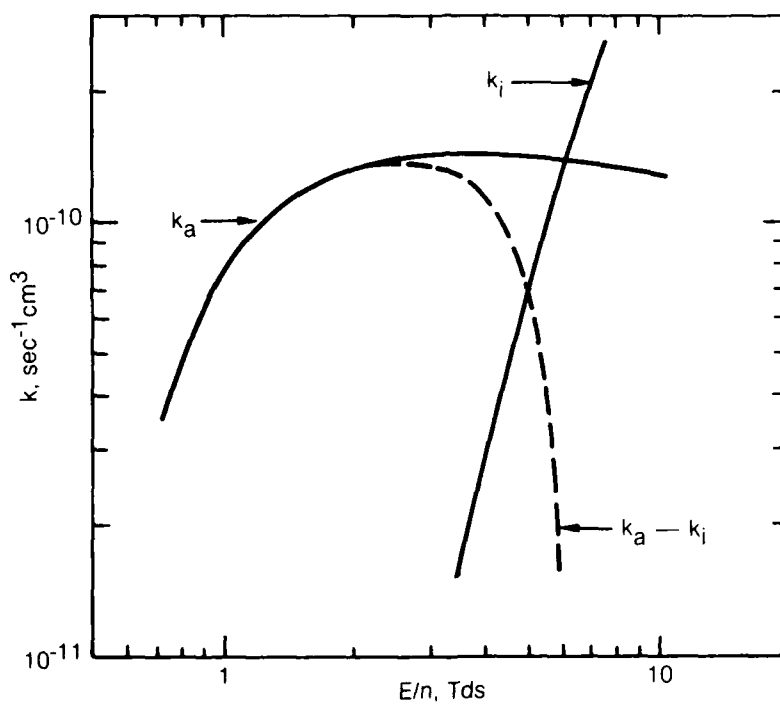
28

Fig. 13 Attachment rate coefficient, k_a, and ionization rate coefficient, k_i, for a Ne – 0.35% $HgBr_2$ mixture computed using the cross sections of Fig. 12 and a fractional ionization value of 2×10^{-6}. Also shown is the difference or net attachment coefficient k_a-k_i.

Numerical experimentation involving variations in both the magnitude and threshold slopes of the cross sections $Q_x(5.0)$, $Q_x(B)$ and $Q_x(7.9)$ indicates that computed laser/discharge properties are rather insensitive to the magnitude and very sensitive to changes in slope. A change of a factor-of-two in the slope above threshold of one of these cross sections has a significant effect on the computed gain, HgBr(B) formation efficiency, and E/n value for which instability occurs, unless a compensating change in the slopes of the other electronic cross sections is made. Thus, the electronic cross sections inferred as described herein must be considered as a set. Nonetheless, the cross sections presented in Fig. 12 were found to provide satisfactory agreement between computed and measured discharge and laser properties for all mixtures and conditions examined in the present investigation. However, with the exception of those for attachment and ionization,[5,23] all the cross sections shown in Fig. 12 are inferred and should be considered provisional pending measurement of the individual e-HgBr$_2$ cross sections.

2. Fractional Power Transfer - Ne-HgBr$_2$

Various contributions to the electron fractional power transfer (FPT) for the Ne-HgBr$_2$ conditions discussed above, computed using the cross sections of Fig. 12, are presented in Fig. 14. Over a relatively broad range of E/n, the FPT associated with HgBr(B) formation is in the 7-8% range for the present conditions, which upon consideration of the quantum efficiency, results in a maximum HgBr(B) formation efficiency of about 3%. Numerical experimentation shows that this value is very sensitive to the slope of $Q_x(B)$ (Fig. 12) because of the blocking effect
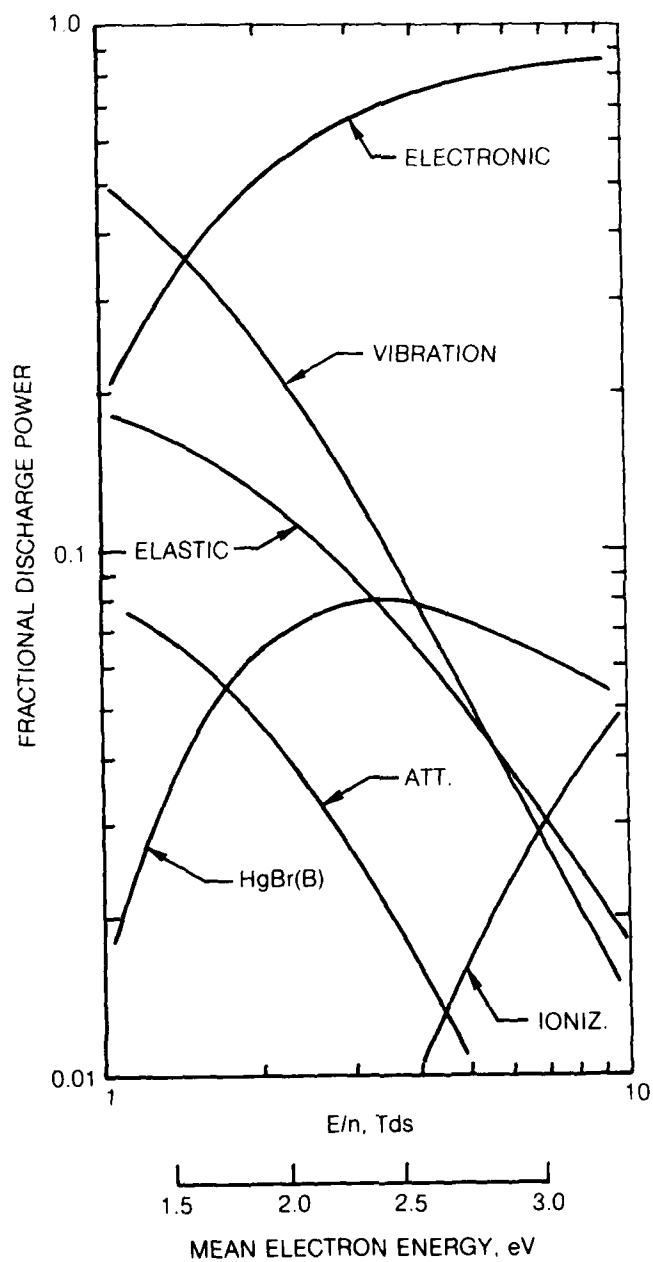
Fig. 14 Various contributions to the electron fractional
power transfer (FPT) for a Ne – 0.35% $HgBr_2$ mixture computed
for the conditions of Fig. 13.

of the 7.9 eV cross section. For these mixture conditions by far the largest contribution to FPT is the combined effect of the 5.0 and 7.9 eV electronic cross sections, particularly the latter. Indeed, with the computed FPT fo the effective 7.9 eV process five-to-ten times larger than that of HgBr(B) formation, it seems highly likely that excitation of higher lying $HgBr_2$ states (as represented by the 7.9 eV process) also contribute significantly to HgBr(B) formation. Even if the HgBr(B) branching fraction associated with the 7.9 eV process is as low as 5%, HgBr(B) formation efficiency and gain will be affected significantly. For this reason, assignment of all HgBr(B) formation to a single cross section, $Q_x(B)$, while convenient, is probably not correct.

Figure 14 also shows that the FPT due to vibrational excitation of $HgBr_2$ is also significant. For the present mixture conditions vibrational excitation represents about a 10% electron energy loss, a value which increases rapidly for lower E/n values. In addition, by depressing the tail of the electron energy distribution, the resonant vibrational cross section, Q_{VR}, significantly affects the magnitude and variation of the attachment coefficient at low E/n values[5] (Fig. 5).

B. Electron-Electron Collisions

Although the electron energy distribution function is non-Maxwellian for the glow discharge conditions typical of the present investigation, the fractional ionization, $\alpha = n_e/n$, is at least 10^{-6} and usually higher. At this fractional ionization level it has been shown[7] that electron-electron collisions exert

32

an important influence on the electron distribution function, particularly the high energy region. All electron transport properties and rate coefficients are affected by the change in the distribution function, most significantly processes having an energy threshold much higher than the 2-3 eV mean electron energy typical of HgBr(B)/HgBr$_2$ laser discharge. As an illustration of the importance of this effect in the present context, Fig. 15 presents the computed fractional ionization dependence of electron drift velocity, the HgBr$_2$ ionization coefficient, and the Ar metastable production coefficient computed for an Ar-0.35% HgBr$_2$ mixture at a constant E/n value of 7 Tds. These results show that processes such as excitation and ionization can exhibit a significant dependence on fractional ionization for values of this variable less than 10^{-6}; even the electron drift velocity changes substantially for $\alpha > 10^{-6}$. Calculations show that the effect of e-e collisions is most pronounced when the background gas has an electron momentum transfer cross section exhibiting a strong energy variation such as Ar. Additionally, the sensitivity of transport properties and rate coefficients to increases in fractional ionization is larger the lower the E/n value, reflecting the strong increase in the cross section for electron-electron collisions with decreasing electron energy[27].

Since the electron distribution function exhibits a dependence on fractional ionization, it is particularly important to include the effect of electron-electron collisions in analyses of discharge conditions for which $\alpha \gtrsim 10^{-6}$. Obviously, electron cross sections inferred on the basis of analysis of e-beam controlled laser/discharge performance will be affected unless the dependence of the electron energy distribution on both E/n _and_ fractional ionization is taken into account.
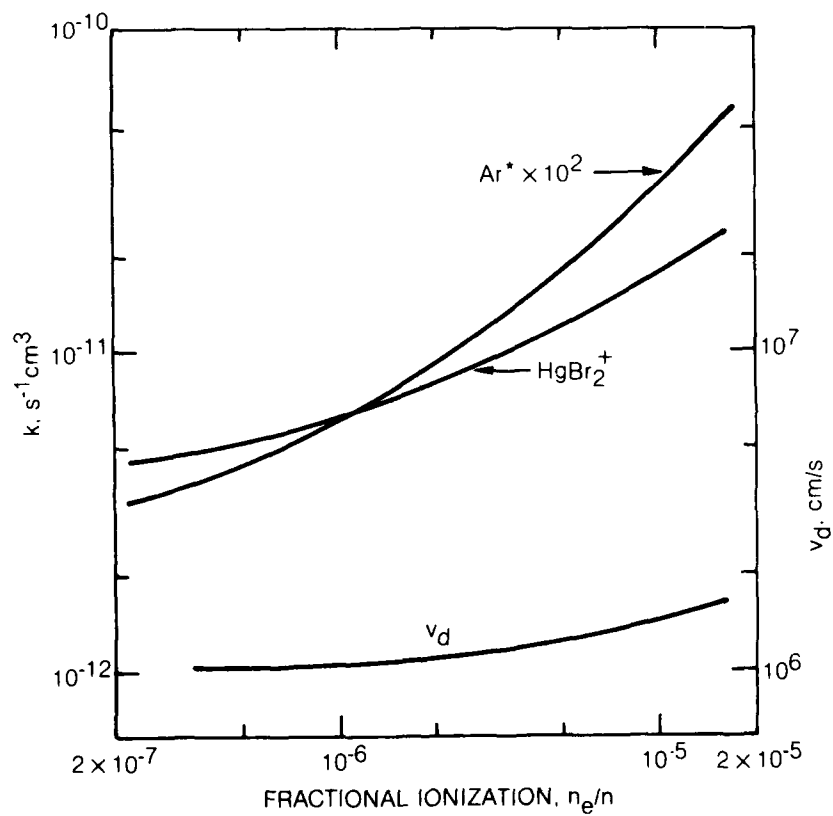
33

Fig. 15 Dependence of the electron drift velocity, v_d, HgBr$_2$ ionization coefficient, and Ar metastable production coefficient on fractional ionization, $\alpha = n_e/n$, computed for an E/n value of 7 Tds. The dependence of these properties on α is stronger for lower E/n values and weaker for higher values.

VI. SUMMARY

In the present investigation measurements of e-beam controlled discharge current density, HgBr(B→X) fluorescence, and 502nm small-signal gain, obtained for several gas mixtures and a large range of E/n values, have been analyzed in detail. Good agreement between measured and computed discharge current density has been obtained, due in large measure to consideration of both vibrational excitation[5] of $HgBr_2$ by low energy electrons, and the influence of electron-electron collisions on the electron energy distribution, and subsequently on computed electron dirft velocity and rate coefficients. Once able to predict discharge current density over a wide range of experimental variables, attention was directed toward analysis of HgBr(B) reaction kinetics. In mixtures comprised of Ne or Ar and $HgBr_2$, direct electron impact dissociative excitation of $HgBr_2$ is found to dominate HgBr(B) formation, a conclusion also reported by other investigators[3,25]. With N_2 or Xe added to the mixture, dissociative excitation transfer dominates HgBr(B) production. In N_2 containing mixtures $N_2(A^3\Sigma_u^+)$ and a higher N_2^* state(s) (probably $B^3\Pi_g$) are reactively quenched by $HgBr_2$ resulting in HgBr(B) formation with branching fractions of 15% and $25\pm5\%$, respectively. Excitation transfer from $Xe(^3P_2)$ following quenching by $HgBr_2$ results in HgBr(B) formation with near unit branching, and is the dominant reaction in mixtures containing Xe. However, for the conditions examined to date a competitive $Xe(^3P_2)$ loss channel appears to significantly limit the efficiency of HgBr(B) formation and thus laser performance. We suggest Ne three-body quenching of the closely coupled $^3P_1$ state

as a likely possibility. In any case, with the exception of Xe mixtures, the present analysis shows that the HgBr(B) formation pathway is not very selective, a factor likely to limit the efficiency of HgBr(B) formation to a maximum value of approximately 5% even under the most optimum of conditions.

In conjunction with a closely related study,[5] a set of self-consistent e-HgBr$_2$ cross sections for attachment, ionization, vibrational excitation and electronic excitation has been determined. When used to model laser/discharge kinetics this cross section set results in satisfactory agreement between measured and computed properties. However, it should be recognized that only the cross sections for HgBr$_2$ ionization and attachment have been actually measured,[5,23] while the cross sections for vibrational and electronic excitation have been inferred on the basis of related experimental observations. Although very useful in the present context, such inferred cross sections should be considered provisional pending the availability of measured cross sections.

REFERENCES

1. R. Burnham and E. J. Schimitschek, Laser Focus 17, 54 (1981).

2. R. T. Brown and W. L. Nighan, Appl. Phys. Lett. 37, 1057 (1980).

3. M. McGeoch, J. Hsia, and D. Klimek, Bull. Am. Phys. Soc. 27, 102 (1982);
   C. H. Fisher, I. Smilanski, T. DeHart, J. P. McDaniel and J. J. Ewing,
   Bull. Am. Phys. Soc. 27, 102 (1982); E. J. Schimitschek and J. E. Celto,
   Appl. Phys. Lett. 36, 176 (1978).

4. W. L. Nighan, in Applied Atomic Collision Physics (H. S. W. Massey,
   E. W. McDaniel and B. Bederson, eds.) Chapter 11, (Academic Press, New York,
   1982); and references cited therein.

5. W. L. Nighan, J. J. Hinchen and W. J. Wiegand, J. Chem. Phys. (to be published).

6. L. Brewer, in The Chemistry and Metallurgy of Miscellaneous Material
   (L. L. Quill, ed.) pp. 183-274 (McGraw-Hill, New York, 1950).

7. W. L. Nighan, IEEE J. Quantum Electron. QE-14, 714 (1978).

8. Techniques used in modeling discharge and laser properties have become well de-
   veloped in recent years in connection with investigations of excimer lasers.
   Specific details of the methods used in the present investigation can be found
   in Refs. 4, 5 and 7 and will not be repeated herein.

9. A. G. Robertson, J. Phys. B: Atom. Molec. Phys. 5, 648 (1972).

10. L. S. Frost and A. V. Phelps, Phys. Rev. 136, A1568 (1964).

11. A. G. Engelhardt, A. V. Phelps and C. G. Risk, Rev. 135, A1566 (1964).

12. R. Johnson and M. A. Biondi, J. Chem. Phys. 73, 5048 (1980).

13. W. Wadt, J. Chem. Phys. 72, 2469 (1980).

14. R. S. F. Chang and R. Burnham, Appl. Phys. Lett. 36, 397 (1980).

15. T. D. Dreiling and D. W. Setser, Chem. Phys. Lett. 74, 211 (1980).

16. T. D. Dreiling, D. W. Setser and S. Ferrero, (to be published).

17. H. Helvajian and C. Wittig, Appl. Phys. Lett. 38, 731 (1981).

18. W. L. Nighan, Appl. Phys. Lett. 36, 173 (1980).

19. D. C. Cartwright, S. Trajmar, A. Chutjian, and W. Williams, Phys. Rev. A. 16, 1041 (1977).

20. H. Horiguchi, R. S. F. Chang and D. W. Setser, J. Chem. Phys. 75, 1207 (1981).

21. R. E. Gleason, T. D. Bonifield, J. W. Keto and G. K. Walters, J. Chem. Phys. 66, 1589 (1977).

22. W. Wieme and J. Lenaerts, J. Chem. Phys. 72, 2708 (1980).

23. W. J. Wiegand and L. R. Boedeker, Appl. Phys. Lett. 40, 225 (1982).

24. J. Degani, M. Rokni and S. Yatsiv, J. Chem. Phys. 75, 164 (1981).

25. J. McGeoch, J. Hsia and D. Klimek (to be published).

26. D. Spence and M. A. Dillon (to be published).

27. I. P. Shkarofsky, T. W. Johnston, and M. P. Bachynski, The Particle Kinetics of Plasmas (Addison-Wesley, Reading, Massachusetts, 1966); Chapter 7.

APPENDIX

Efficient HgBr(B→X) Laser Oscillation in Electron-Beam
Controlled-Discharge-Excited Xe/HgBr$_2$ Mixtures

by
Robert T. Brown and William L. Nighan

Efficient HgBr (B→X) laser oscillation in electron-beam-controlled-discharge-excited Xe/HgBr₂ mixtures

Robert T. Brown and William L. Nighan

United Technologies Research Center, East Hartford, Connecticut 06108

This letter reports the results of an investigation of HgBr($B\,^2\Sigma^+ \to X\,^2\Sigma^+$) laser oscillation at 502 nm in Xe-HgBr₂ mixtures excited using an electron-beam-controlled discharge. Measured values of instantaneous electrical-optical energy conversion efficiency were 2%, a level substantially higher than that typical of N₂-HgBr₂ mixtures. Calculations show that efficiencies of 5–10% may be possible under optimized conditions.

The HgBr($B\,^2\Sigma^+ \to X\,^2\Sigma^+$) laser operating at 502 nm promises to be an important optical source in the blue/green region of the spectrum. Excitation of this laser transition has been achieved by dissociative excitation of the mercuric-bromide molecule, HgBr₂, in an electric discharge.[1] Using N₂-HgBr₂ mixtures, electrical-optical energy conversion efficiencies in the 0.5–1.0% range have been obtained.[1] Analysis of the kinetics of electrically excited N₂-HgBr₂ mixtures has shown that the HgBr($B\,^2\Sigma^+$) laser molecule is formed following predissociation of HgBr₂($^1\Sigma_u^+$), the latter produced as a result of N₂($A\,^3\Sigma_u^+$) quenching by HgBr₂ molecules.[1] However, calculations show that the production efficiency of N₂($A\,^3\Sigma_u^+$) in N₂-HgBr₂ discharges is about 10–15%, and recent measurements indicate that the N₂($A\,^3\Sigma_u^+$)-HgBr₂ branching fraction for HgBr($B\,^2\Sigma^+$) formation is only 15–20%.[1] These factors may limit the efficiency of the discharge-excited HgBr(B)/HgBr₂ dissociation laser to a value of approximately 1% when N₂ is used as the energy transfer molecule.

By way of contrast, recent measurements show that the Xe($^1P_2$) metastable atom has a large rate coefficient for HgBr₂ dissociative excitation and that HgBr($B\,^2\Sigma^+$) is formed with near unit efficiency.[4] In addition, the present calculations show that Xe($^1P_2$) metastable atoms can be produced with high efficiency (> 50%) over a broad range of electric discharge conditions. For these reasons Xe has unusual potential as an energy transfer species in the HgBr(B)/HgBr₂ dissociation laser. In this letter we report the results of efficient HgBr($B \to X$) laser oscillation in Xe-HgBr₂ mixtures using an electron-beam-controlled discharge.

The present experiments were carried out using a $1.5 \times 1.7 \times 50$-cm active volume within the heated discharge cell shown schematically in Fig. 1. Previous investigations[5] have shown that proper cell design is critical in order to maintain chemical purity of the gas mixture. In order to keep HgBr₂-surface interactions to a minimum, in this cell the only materials in contact with the working gas mixture were type 316 stainless-steel, Pyrex, Kalrez, and dielectric-coated mirrors. HgBr₂ crystals were contained in a Pyrex reservoir positioned in a side arm as shown in the figure. Variation of the cell (and reservoir) temperature in the 150–200 °C range provided a corresponding variation in HgBr₂ partial pres-

sure from about 1 Torr to approximately 15 Torr. The electron beam system and discharge driver utilized in this investigation have been described previously.[5]

Presented in Fig. 2 are representative measured characteristics for a mixture containing 10% Xe in a Ne buffer at a total pressure of 2 atm and a temperature of 185 °C. Based on available vapor pressure data,[7] the HgBr₂ concentration for these conditions was 2.4×10^{17} cm⁻³, corresponding to a mixture fraction of approximately 0.007. In this case the electron beam was initiated 200 ns before the discharge voltage and provided a constant e-beam current density of 0.5A cm⁻² for 1.2 μsec. The discharge voltage was provided by a low-inductance capacitor of a size so as to produce only a very slight decrease in voltage (i.e., E/n) during the pulse. With this arrangement it was possible to produce a highly uniform plasma medium which was essentially quasisteady. For the conditions of Fig. 2 the measured current and voltage exhibited essentially steady-state behavior for over 0.5 μsec, at which time the discharge was terminated by arcing.

Time-dependent discharge and laser properties were modeled numerically using procedures which have been described previously.[3,6] Computed current-voltage characteristics were found to be in very good qualitative and quantitative agreement with measured values over a range of E/n values and HgBr₂ concentrations. In addition, the onset of arcing could be predicted and was shown to be due to volu-
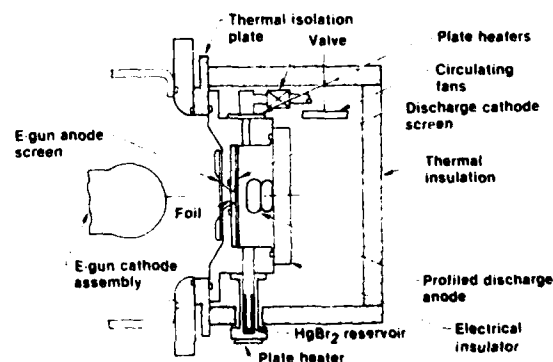

FIG. 1 Illustration of heated HgBr(B)/HgBr₂ laser discharge cell

Discharge
current density ⎯⎯⎯⎯ 14 A·cm⁻²

Discharge E/n ⎯⎯⎯⎯ 0.65 × 10⁻¹⁶ V·cm²

HgBr(B→X)
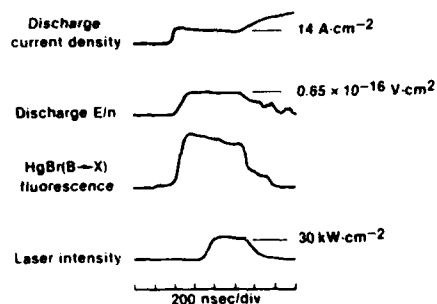fluorescence

Laser intensity ⎯⎯⎯⎯ 30 kW·cm⁻²

200 nsec/div

FIG. 2. Representative characteristics for an e-beam-controlled-discharge-excited mixture comprised of 10% Xe in a Ne buffer at a total pressure of 2 atm and a temperature of 185 °C. For these conditions the HgBr₂ concentration in the cell was 2.4×10^{17} cm⁻³, approximately 0.7% of the total mixture. The e-beam current density (at the center of the discharge) was 0.5 A·cm⁻².

metric ionization instability.[6] Prior to the onset of arcing the discharges were found to operate in a high-impedance (2-3 Ω), externally controlled mode. Modeling of discharge properties indicated that for conditions typical of this investigation (e.g., Fig. 2) 80–90% of the deposited energy was provided by the discharge, and 60–70% of the ionization was provided by the e-beam, values found to be consistent with experimental observations. Thus the Ne/Xe/HgBr₂ discharges examined in this investigation were e-beam *controlled* and exhibited a high discharge:e-beam *energy enhancement factor*.

The HgBr₂($B\,^2\Sigma^+ \to X\,^2\Sigma^+$) fluorescence was found to be a relatively sensitive function of applied voltage, reflecting the strong dependence of Xe($^3P_2$) metastable production of E/n. Modeling of discharge characteristics indicated that HgBr($B\,^2\Sigma^+$) was produced with an efficiency typically in the 15–20% range by way of the reaction sequence[8]

$$e \xrightarrow{\text{Xe}} \text{Xe}(^3P_2) \xrightarrow{\text{HgBr}_2} \text{HgBr}(B\,^2\Sigma^+).$$
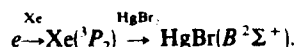
Computed zero-field gain based on the calculated HgBr ($B\,^2\Sigma^+$) concentration and using a stimulated emission cross section of 2.4×10^{-16} cm² was approximately 0.03 cm⁻¹ for the conditions of Fig. 2.

Using an internally mounted optical cavity consisting of a 4.0-m max R mirror and a flat 90% R output coupler, the laser pulse shown in Fig. 2 was obtained. The output beam imaged the full 1.5×1.7-cm discharge cross section and was found to be very uniform. Although the onset of laser oscillation was delayed, Fig. 2 shows that a uniform laser pulse of almost 400-nsec duration was obtained. More-

over, the instantaneous electrical-optical energy conversion efficiency was found to be 2.0%, a level substantially higher than that typical of N₂/HgBr₂ laser mixtures. However, calculations show that in the absence of appreciable volumetric absorption (i.e., for gain/absorption ratios greater than 10) laser efficiencies greater than 5% should be attainable for these conditions. Both the delayed onset and the apparently low optical extraction efficiency are suggestive of a *net* gain lower than the computed value, and/or a relatively high level of volumetric absorption. With an HgBr₂ concentration in excess of 10^{17} cm⁻³, even a low level of surface reactions and/or impurities introduced with the HgBr₂ could result in a substantial level of neutral impurities, one or more of which may either absorb at the laser wavelength or quench HgBr(B). Additionally, ionic or excited states of HgBr₂ itself may absorb in the blue/green region of the spectrum. These possibilities are presently being studied in more detail.

The present investigation has shown that use of Xe as the primary energy receptor-transfer species in e-beam-controlled-discharge-excited HgBr(B)/HgBr₂ dissociation lasers permits laser efficiency higher than reported for N₂-HgBr₂ mixtures. More importantly, calculations show that electrically excited Xe-HgBr₂ mixtures have the potential for development as blue/green sources with efficiencies even higher than those measured in the present experiments. Modeling of discharge/laser properties for a variety of conditions suggests that electrical-optical energy conversion efficiencies of 5–10% may be possible under optimized conditions.

[1] E. J. Schimitschek and J. E. Celto, Appl. Phys. Lett. **36**, 176 (1980), and references cited therin.
[2] W. L. Nighan, Appl. Phys. Lett. **36**, 173 (1980).
[3] T. D. Dreiling and D. W. Setser, Chem. Phys. Lett. (to be published).
[4] R. S. F. Chang and R. Burnham, Appl. Phys. Lett. **36**, 397 (1980).
[5] E. J. Schimitschek and J. E. Celto, Opt. Lett. **2**, 64 (1978).
[6] R. T. Brown and W. L. Nighan, Appl. Phys. Lett. **32**, 730, 1978; **35**, 144 (1979).
[7] L. Brewer, in *The Chemistry and Metallurgy of Miscellaneous Material*, edited by L. L. Quill (McGraw-Hill, New York, 1950).
[8] Experimentation with neon-HgBr₂ mixtures yielded evidence of a direct HgBr(*B*) formation mechanism tentatively identified as electron impact dissociative excitation of HgBr₂. The magnitude of the rate coefficient for this process, which is required to explain the experimental observation of HgBr(*B→X*) fluorescence in neon-HgBr₂ mixtures, suggests that a direct electron excitation of HgBr₂ resulting in HgBr(*B*) may also be significant reaction in mixtures containing either N₂ or Xe.

41

R82- 925096-1

April 29, 1982

Initial Distribution List

Director, Physics Program (Code 421)   1 copy
Office of Naval Research   (with DD250)
800 North Quincy Street
Arlington, Virginia 22217

Attn: Dr. M. B. White
Ref.: Contract N00014-80-C-0247
      Project: NR395-711/12-19-80

Air Force Plant Representative Office   1 copy
Pratt & Whitney Aircraft, O.L.-AA
East Hartford, CT 06108

Ref.: Contract N00014-80-C-0247
      Project: NR395-711/12-19-80

Director, Naval Research Laboratory   6 copies
Code 2627
Washington, D. C. 20375

Defense Technical Information Center   12 copies
Bldg. 5, Cameron Station
Alexandria, Virginia 22314

Office of Naval Research   1 copy
Eastern/Central Regional Office
Boston, Mass 02210

Additional Copies

Dr. E. J. Schimitschek   1 copy
Code 811
Naval Ocean Systems Center
271 Catalina Blvd.
San Diego, CA 92152

Dr. R. Burnham   1 copy
Laser Physics Branch
Naval Research Laboratory
Washington, D. C. 20375

Distribution List (Cont'd)

Dr. R. E. Behringer
Office of Naval Research   1 copy
1030 East Green Street
Pasadena, CA 91101

Dr. H. S. Pilloff
Physics Program (Code 421)   1 Copy
Office of Naval Research
800 North Quincy Street
Arlington, VA 22217